QUANTIFICATION OF PULMONARY VEIN MORPHOLOGY USING CENTERLINE TRACKING

M.E. Rettmann[1], M.S. Gunawan[3], D.R. Holmes III[1], D.L. Packer[2], R.A. Robb[1]

[1]Biomedical Imaging Resource, [2]Division of Cardiology/Electrophysiology,
Mayo Clinic College of Medicine, Rochester, MN, USA
[3]Department of Biochemistry and Molecular & Cellular Biology
Georgetown University, Washington D.C., USA

ABSTRACT

The assessment of left atrial and pulmonary vein morphology has important applications in the context of atrial fibrillation, a condition in which the atria of the heart beat rapidly and irregularly. Following ablation therapy, a treatment strategy for atrial fibrillation, reverse structural remodeling has been demonstrated with decreases in both left atrial size and pulmonary vein diameters. Most techniques for assessment of pulmonary vein morphology, however, consist of manual measurements made on cross-sectional images or volume renderings, thereby limiting the ability to fully quantify the 3D structure of the veins. In this work, we propose a method to quantify the 3D morphology of the pulmonary veins by computing the cross-sectional area along the entire extent of the vein. A centerline is tracked along the vein and oblique image slices are extracted at each point along the curve. The overall method requires only minimal manual interaction during the data pre-processing steps and is demonstrated on each of the four pulmononary veins in five subjects scanned with CT imaging prior to ablation therapy.

Index Terms— pulmonary veins, cardiac ablation therapy, left atrial fibrillation, centerline tracking

1. INTRODUCTION

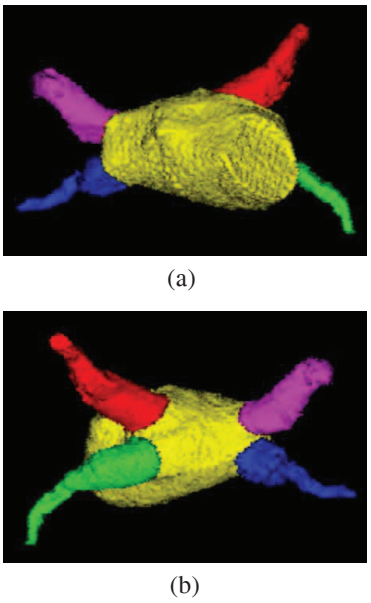
The assessment of left atrial and pulmonary vein morphology has important applications in the context of atrial fibrillation, a condition in which the atria of the heart beat rapidly and irregularly. Patients with atrial fibrillation have been shown to have increased left atrial volumes and pulmonary vein diameters, a process called structural remodeling. Following ablation therapy, a treatment strategy for atrial fibrillation, reverse structural remodeling has been demonstrated with decreases in both left atrial size and pulmonary vein diameters [1, 2, 3]. Efforts have been made to quantify pulmonary vein structure [4, 5], however, most techniques consist of manual measurements made on cross-sectional images or volume renderings, thereby limiting the ability to fully quantify the 3D structure of the veins. In previous work by ourselves and others [6, 7], the pulmonary veins have been modeled using a centerline curve and oblique image sections. Our previous work focussed on automatic detection of the junction between the left atrium and pulmonary veins. The focus of the current work is a robust methodology for 3D quantitative assessment of pulmonary vein structure in the application of cardiac ablation therapy.

This research was supported by NIH grants HL089709 and HL089645 from the National Heart Lung and Blood Institute and EB002834 from the National Institute of Biomedical Imaging and Bioengineering.

2. METHODS

The first step is to segment the left atrium and pulmonary veins from CT imaging data using a semi-automatic method based on a previously described technique [8, 9]. In the segmentation process, the left atrium and pulmonary veins are first segmented as a single structure using thresholding and region growing operations. Next the pulmonary veins are separated from the left atrium by the user interactively positioning a cut plane at the juction between the left atrium and pulmonary vein, called the pulmonary vein ostium. In the current application, only the main branch of the pulmonary vein is segmented, all side branches are manually removed from the segmentation. A sample segmentation is shown in Figure 1 with the pulmonary veins segmented separately from the left atrium. The proximal endpoint for centerline tracking in each pulmonary vein is computed as the centroid of the boundary between the segmented left atrium and the pulmonary vein. The distal endpoint is selected manually by the user using a volumetric display.

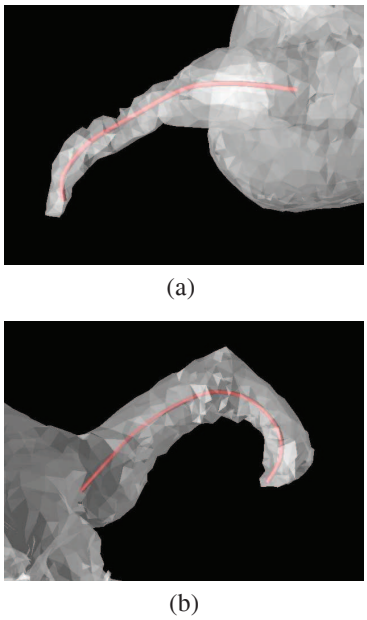
Centerline tracking along each pulmonary vein is accomplished using a series of steps. First, the binary segmentation of a single pulmonary vein is smoothed using a series of morphological operations. If the endpoints are removed from the binary volume during the smoothing operation, the closest voxel in the foreground is found and used as that endpoint. The centerline tracking algorithm follows a previously



(a)

(b)

Fig. 1. Segmented left atrium and pulmonary veins from (a) front and (b) back views. Left atrium (LA) in yellow, left inferior pulmonary vein (LIPV) in green, left superior pulmonary vein (LSPV) in red, right inferior pulmonary vein (RIPV) in blue, right superior pulmonary vein (RSPV) in magenta.



(a)

(b)

Fig. 2. Centerlines tracked for the (a) left inferior and (b) right superior pulmonary veins.

described method [10] in which the skeleton of the object is computed and the shortest path between endpoints is found using a simplified version of Djistra's shortest path. In order to prevent the centerline from traversing side loops often created in the skeleton algorithm, a weighted skeleton is computed by multiplying the binary skeleton with the inverse of the distance transform from the boundary of the segmented binary object. This gives voxels closer to the center of the object smaller values and voxels in side loops larger values. A weighted Djikstra's shortest path algorithm is then used which backtracks along the minimal path from the distal endpoint to the proximal endpoint. The result of the path traversing algorithm is a curve which runs along the center of the pulmonary vein. This path may, however, still contain sharp bends. In order to create a smooth path, the centerline is subsampled and a spline is fit to these points. The resulting centerlines tracked for the left inferior and right superior pulmonary veins are shown in Figure 2.

In order to measure the cross-sectional area along the length of the pulmonary vein, oblique image slices are extracted between points of the spline curve by computing the unit vector between the current point and the next point and using the vector and current point to define an oblique plane. The oblique plane is used to cut the pulmonary vein and the the cross-sectional area is measured at that point. Cumulative distance along the pulmonary vein is computed as a piecewise addition of distances between curve points. Since pulmonary veins may enter the left atrium at a large angle, it is possible for the oblique slice to underestimate the cross-sectional area near the pulmonary vein ostia, as demonstrated in Figure 3. As shown in Figures 3(a) and (b), the oblique to the centerline close to the right superior pulmonary vein ostium is an image slice cutting across both the pulmonary vein and the left atrium. Since only the area in the pulmonary vein is measured, this may underestimate the cross-sectional area at this point. A more accurate measurement of the cross-sectional area near the pulmonary vein ostium could be obtained using the manually adjusted cut plane used for separating the pulmonary veins from the left atrium during the segmentation process (see Figures 3(c) and (d)). The orientation of this plane, however, would not accurately represent the cross-sectional area further into the pulmonary vein, particularly in veins with large bends.

To addresss this issue, the orientation of the oblique image used for measuring the cross-sectional area is computed using a combination of the centerline oblique and the orientation of the manually adjusted cut plane used for segmentation as follows:

$$\mathbf{v_3} = \alpha_1 \mathbf{v_1} + \alpha_2 \mathbf{v_2} \tag{1}$$

where $\alpha_1 + \alpha_2 = 1$ and $\alpha_1 = \frac{1}{c^n}$. $\mathbf{v_3}$ is the new normal vector defining the oblique plane, $\mathbf{v_1}$ is the normal from the segmentation cut plane and $\mathbf{v_2}$ is the normal vector defined by the centerline. c is a constant and n is the point along the curve. In this work, c is set to 1.1 and held fixed for all datasets. The result of equation (1) is that the initial obliques are weighted heavily by the segmentation cut plane

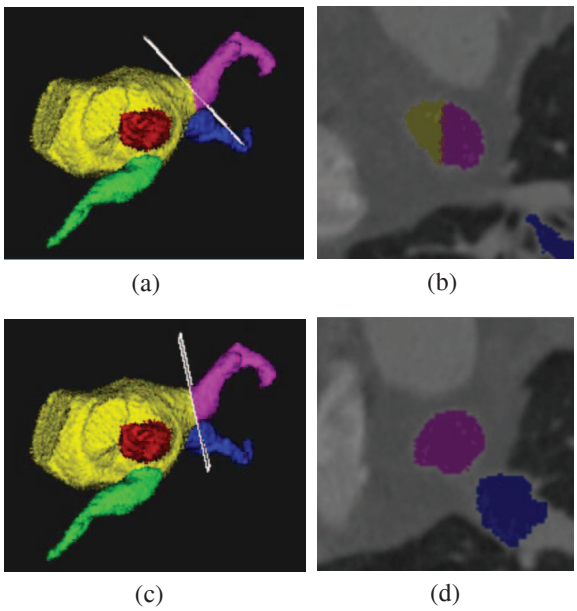


Fig. 3. The oblique to the centerline near the right superior pulmonary vein (a) and its associated image cross-section (b). The manually adjusted cut plane used to separate the pulmonary vein from the left atrium during the segmentation process (c) and its associated image cross-section (d).

with this effect falling off quickly as the centerline travels down the pulmonary vein. This is demonstrated in Figure 4 which shows the cross-sectional area along the extent of the four pulmonary veins by extracting either the oblique to the centerline normal, the segmentation cut-plane normal, or the normal computed as a combination of the two vectors. Focussing on the right superior pulmonary vein, the segmentation cut-plane normal gives an accurate cross-sectional area near the pulmonary vein ostia, however, it quickly overestimates the cross-sectional area once the pulmonary veins starts to bend. The centerline oblique appears to initially underestimate the cross-sectional area, and the combined approach provides a reasonable measurement along the entire extent of the vein.

As a final step in the process, a procedure is employed to reduce the dependence of the centerline curve on the proximal endpoint. Twenty-five endpoints are randomly selected on the intersecting plane between the left atrium and pulmonary vein. Each of the endpoints are restricted to lie within 3 mm of the plane's centroid. The centerline tracking is run for each of the endpoints and a mean curve is computed from all trials.

3. RESULTS

The proposed methodology is demonstrated on each of the four pulmononary veins in five subjects scanned using CT

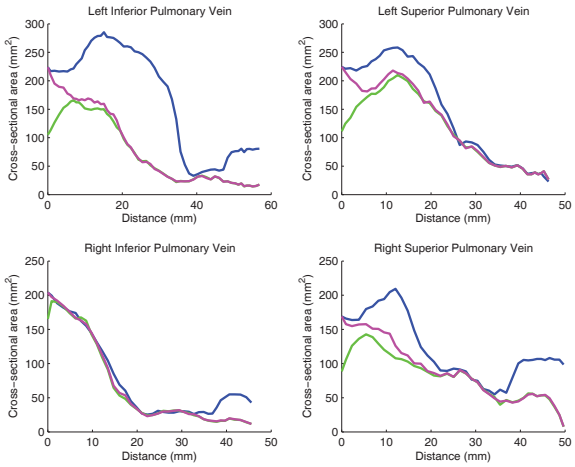


Fig. 4. Cross sectional area versus distance along each of the four pulmonary veins computed using three methods: (1) Oblique computed from the normal to the centerline curve (green), oblique computed from the normal of the cut plane used during the segmentation process (blue), and oblique computed from the normal computed as a combination of the two vectors (magenta).

imaging prior to ablation therapy. In Figure 5, the cross-sectional area is plotted along the length of each pulmonary vein where each subject is shown in a different color. These plots demonstrate a high variability across subjects near the pulmonary vein ostia, with this variability decreasing near the distal end. The left superior pulmonary vein demonstrates the largest amount of variability at the ostium and the left inferior pulmonary vein has the tightest spread of cross-sectional area measurements near the ostium. The area of the left superior and inferior and right superior tend to decrease rapidly during the first 4 cm while the right inferior tends to asymptote earlier, closer to 2 cm. In addition, several of the curves show an initial decrease in cross-sectional area, followed by plateau and then another rapid decrease in area.

4. DISCUSSION

In this work, a new methodology is proposed to quantitatively assess morphology of the pulmonary veins which has become increasingly important in the context of left atrial fibrillation and ablation therapy. It has been shown that anatomical reverse remodeling occurs in patients undergoing ablation therapy, with decreases in both left atrial size and pulmonary vein diameters. The pulmonary vein measurements, however, are typically restricted to 2D image cross-sections or manual measurements on volume renderings. In addition, while decreases in diameters have been observed at the pulmonary vein ostia, it is not yet understood how far into the pulmonary vein this remodeling occurs. We are currently working to ap-

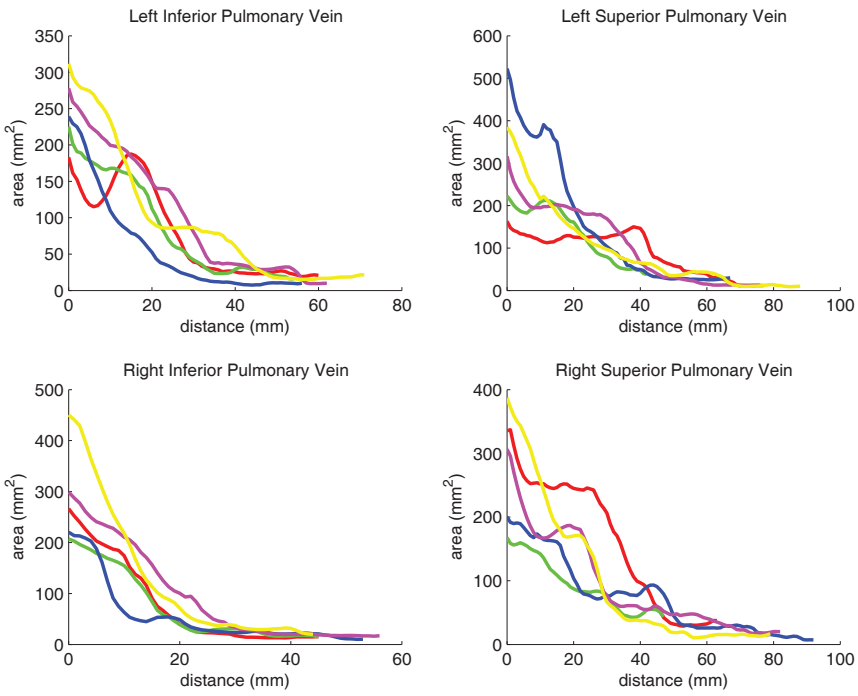


Fig. 5. Result of applying the proposed methodology to each of the four pulmonary veins in 5 subjects. Cross-sectional area in mm^2 is plotted versus distance along the pulmonary vein in mm. Each subject is shown in a separate color.

ply this technique to a series of patients scanned both before and three months following a cardiac ablation procedure. This will provide important insight into the extent of reverse structural remodeling that occurs along the entire length of the pulmonary veins in response to this therapy.

5. REFERENCES

[1] K. Lemola et. al., "Effects of left atrial ablation of atrial fibrillation on size of the left atrium and pulmonary veins," *Heart Rhythm*, vol. 1, pp. 576–581, 2004.

[2] V.K. Jayam et. al., "Atrial volume reduction following catheter ablation of atrial fibrillation and relation to reduction in pulmonary vein size: an evaluation using magnetic resonance angiography," *J Interv Card Electrophysiol*, vol. 13, no. 2, pp. 107–14, 2005.

[3] H.-M. Tsao et. al., "Morphologic remodeling of pulmonary veins and left atrium after catheter ablation of atrial fibrillation: Insight from long-term follow-up of three-dimensional magnetic resonance imaging," *J Cardiovasc Electrophysiol*, vol. 16, pp. 7–12, 2005.

[4] Y-H. Kim et. al., "Pulmonary vein diameter, cross-sectional area, and shape: CT analysis," *Radiology*, vol. 235, pp. 43–50, 2005.

[5] M. Ueda et. al., "Pulmonary vein morphology before and after segmental isolation in patients with atrial fibrillation," *PACE*, vol. 28, pp. 944–953, 2005.

[6] R. Karim et. al., "Left atrium pulmonary veins: Segmentation and quantification for planning atrial fibrillation ablation," in *Proceedings of SPIE – Volume 7261*, 2009.

[7] M.E. Rettmann et. al., "Identification of left pulmonary vein ostia using centerline tracking," in *Proceedings of SPIE Medical Imaging*, 2009.

[8] M.E. Rettmann et. al., "Validation of semi-automatic segmentation of the left atrium," in *Proceedings of SPIE*, 2008.

[9] M.E. Rettmann et. al., "Validation of geometric measurments of the left atrium and pulmonary veins for analysis of structural remodeling following ablation therapy," in *Proceedings of SPIE*, 2012.

[10] R.J.T. Sadleir and P.F. Whelan, "Fast colon centreline calculation using optimised 3D topological thinning," *Computerized Medical Imaging and Graphics*, vol. 29, pp. 251–258, 2005.